

## Article

# Assessing the Effectiveness of an Innovative Thermal Energy Storage System Installed in a Building in a Moderate Continental Climatic Zone

Luis Coelho <sup>1</sup>, Maria K. Koukou <sup>2,\*</sup>, John Konstantaras <sup>2</sup>, Michail Gr. Vrachopoulos <sup>2</sup>, Amandio Rebola <sup>1</sup>, Anastasia Benou <sup>3</sup>, Constantine Karytsas <sup>3</sup>, Pavlos Tourou <sup>4</sup>, Constantinos Sourkounis <sup>4</sup>, Heiko Gaich <sup>5</sup> and Johan Goldbrunner <sup>5</sup>

- <sup>1</sup> MARE—IPS—Marine and Environmental Sciences Centre, Escola Superior de Tecnologia, Instituto Politécnico de Setúbal, Campus do IPS—Estefanilha, 2910-761 Setúbal, Portugal; luis.coelho@estsetubal.ips.pt (L.C.); amandio.rebola@estsetubal.ips.pt (A.R.)
- <sup>2</sup> Energy and Environmental Research Laboratory, Evripus Campus, National and Kapodistrian University of Athens, 34400 Psachna, Evia, Greece; yiannis.konstantaras@gmail.com (J.K.); mgrvrachop@uoa.gr (M.G.V.)
- <sup>3</sup> Centre for Renewable Energy Sources and Saving (CRES), Marathonos 19th Km, 19009 Pikermi, Greece; abenou@cres.gr (A.B.); kkari@cres.gr (C.K.)
- <sup>4</sup> Institute for Power Systems Technology and Power Mechatronics, Ruhr-University Bochum, 44801 Bochum, Germany; tourou@enesys.ruhr-uni-bochum.de (P.T.); sourkounis@enesys.ruhr-uni-bochum.de (C.S.)
- <sup>5</sup> Geoteam Technisches Büro für Hydrogeologie, Geothermie und Umwelt GMBH, Bahnhofguertel 77/4, 8020 Graz, Austria; heiko.gaich@zt-neubauer.at (H.G.); je.goldbrunner@gmail.com (J.G.)
- \* Correspondence: mkoukou@uoa.gr; Tel.: +30-2228021846

**Abstract:** In the present work, the operating results from an innovative, renewable, energy-based space-heating and domestic hot water (DHW) system are shown. The system used solar thermal energy as its primary source and was assisted by a shallow geothermal application in order to accommodate the space-heating and DHW needs of a domestic building in Austria. The system incorporated phase-change materials (PCMs) in specially designed containers to function as heat-storage modules and provide an energy storage capability for both the space-heating and DHW subsystems. This system was designed, implemented, and tested under real operating conditions in a building for a period of one year. The operating and energy results for the system are demonstrated in this work. The system was compared with a conventional one, and a reduction in the primary energy consumption equal to 84.3% was achieved. The maintenance and operating costs of the system were reduced by 79.7% compared to the conventional system, thus significantly contributing to the NZEB target of the building. The newly proposed system, although presenting an increased operating complexity, utilizes an innovative self-learning control system that manages all of its operations. The combination of a solar thermal energy source with thermal energy storage increases the use of renewable energy by extending the capacity of the system beyond the solar hours and using excess solar energy for space-heating needs. The thermal energy storage unit also increases the energy and economic efficiency of the geothermal heat pump by operating it during the hours of a reduced electricity tariff and using the stored energy during hours of a high electricity demand. The cost for the installation of such a system is higher than a conventional one, but due to the significantly decreased operating costs, the pay-back period was calculated to be 8.7 years.

**Keywords:** thermal energy storage; solar; geothermal; phase-change materials; space heating; domestic hot water



**Citation:** Coelho, L.; Koukou, M.K.; Konstantaras, J.; Vrachopoulos, M.G.; Rebola, A.; Benou, A.; Karytsas, C.; Tourou, P.; Sourkounis, C.; Gaich, H.; et al. Assessing the Effectiveness of an Innovative Thermal Energy Storage System Installed in a Building in a Moderate Continental Climatic Zone. *Energies* **2024**, *17*, 763. <https://doi.org/10.3390/en17030763>

Academic Editor: Francesco Calise

Received: 12 December 2023

Revised: 29 January 2024

Accepted: 30 January 2024

Published: 5 February 2024



**Copyright:** © 2024 by the authors. Licensee MDPI, Basel, Switzerland. This article is an open access article distributed under the terms and conditions of the Creative Commons Attribution (CC BY) license (<https://creativecommons.org/licenses/by/4.0/>).

## 1. Introduction

### 1.1. Literature Review

The increased energy expenditure and the problems derived from the effects of global warming, in conjunction with the dependency of the European Union on energy imports,

are the main driving forces behind efforts to enhance sustainable energy development and utilize renewable energy sources (RESs) [1–3]. Since 2021, new buildings in the EU must be nearly zero-energy buildings (NZEBs), for which the low energy needs will be covered using RESs [3]. In order to achieve such a goal, it is necessary to find new ways to save energy in buildings and implement renewable energy solutions [3–7]. The use of solar energy applications in the residential sector to cover heating, cooling, and DHW needs has increased; however, there are still issues to consider. Among the challenges due to the time-dependency of solar energy resources, it is necessary to find ways to synchronize the energy demand and supply. Thermal energy storage (TES) is one way, as it allows energy to be stored for use when sunshine is not available [8]. TES has been employed in many heating and industrial systems to enhance their thermal performance [9,10], as it can support the integration of high renewable energy shares in buildings and industry. Another RES, shallow geothermal energy, is used today to cover the heating and cooling loads in buildings. This can be achieved by coupling a ground source heat pump (GSHP) with the ground by means of borehole heat exchangers (BHEs). However, there is a weak point in BHE systems; heat transfer in the ground is mainly conductive, with a low thermal diffusivity, and the ground thermal response is quite low, which results in a lower coefficient of performance (COP) for GSHPs. This issue can be tackled by mixing phase-change materials (PCMs) with backfill material [11,12].

The use of solar and geothermal energy coupled with thermal energy storage in order to cover residential building needs for heating, cooling, and DHW was attempted for the first time in the TESSe2b project [13]. Compact, modular, high-energy-density TES tanks were designed and constructed to store energy in residential buildings for space-cooling (CTES tanks), space-heating (HTES tanks), and domestic hot water (DHW tanks) needs. The TES tanks were built using an innovative stackable design shape in order to easily integrate them into buildings with a small available space. Additionally, the BHEs were enhanced with PCMs in order to improve the TESSe2b efficiency [11]. An advanced control that assisted the system-wide optimization of the components and their operation was developed and had a key role in the optimal charge/discharge cycles of the TESSe2b solution and the overall efficiency. Despite the experimental analysis of PCMs existing in the literature [10,14], an integrated-PCM thermal energy storage system for heating/cooling and DHW, coupled with a control system to optimize the performance, is innovative. In addition, although PCMs are used for heat storage in buildings by integrating them into various materials and construction systems, they have not been used in BHEs so far. The effects of adding PCMs to the ground grout for BHEs and the impact of this was a main objective of the TESSe2b project [13]. Initially, the TESSe2b components were tested on a small scale, and then they were tested on a realistic scale under laboratory conditions [15–17]. Subsequently, the TESSe2b solution was piloted in residential buildings in the following countries: Austria, Cyprus, and Spain. The Cyprus climate is similar to the hot climate that exists in Europe, and it was used as an indicator for cooling needs. The climate of Austria was used as an indicator for the heating needs, while the Spanish climate is characterized by hot, dry summers and mild, rainy winters. In a previous research paper [18], the results from the implementation of TESSe2b in Cyprus, in a building located in a Mediterranean climate in the Paphos region, were shown. In this work, an assessment of the effectiveness of TESSe2b when it is installed in a building in Austria, where heating needs prevail due to the conditions of the moderate continental climatic zone, was attempted.

### 1.2. System Description

Using the Design Builder<sup>®</sup> V4.0 software [19], the building energy needs were calculated, while the critical quantities were calculated based on the results from the TESSe2b implementation in the building. According to the results, TESSe2b reduced the equivalent primary energy needs for heating and DHW when compared with the conventional system used in Austria (boiler and burner using heat oil) for heating and DHW. Furthermore, a

PCM was used as a thermal buffer injected into the BHEs. The PCM was not mixed with the grouting, as is the usual practice; instead, it was inserted into one of the two U-tubes of the BHEs (with the other used for heat transfer fluid (HTF) circulation). The objective of this method was to increase the thermal inertia of the BHEs when their temperature drops below the operating (phase-change) temperature of the PCM, thus improving the COP of the GSHP. Additionally, because the PCM was enclosed in the watertight U-tube, the soil contamination risk was diminished. Although BHEs with a PCM were installed and tested, it was not possible to confirm their advantages, in accordance with what was verified in CFD numerical simulations. To better verify whether there are significant advantages, it will be necessary to install a more complete data acquisition system, involving the evaluation of more parameters, and with the possibility of varying the operating conditions of the geothermal heat pump system and collecting measurements over a prolonged period of time (at least 1 year).

## 2. TESSe2b Implementation in Austria

### 2.1. Research Steps

A full description of TESSe2b is provided in [13,18]. The aim of the research in this work was to evaluate the TESSe2b system's integration into a building in a moderate continental climatic zone, to assess the impact of the solution on the building's energy performance, and to provide evidence about its overall technical and economic feasibility. The steps followed for the research work comprised the following (Figure 1):

1. TESSe2b dimensioning: Work was carried out for the proper dimensioning of the system to cover the needs of the building.
2. Site preparation: It was necessary for the geothermal installation to find and collect data about the geology of the site, evaluate the geology and physical properties of the rocks, and suggest a drilling method to be used on the site. Then, technical and geological supervision of the works was conducted, as well as geological drilling support and an analysis of the geophysical borehole logging.
3. TESSe2b prototype installation in the test building: During this step, all the necessary equipment and components of TESSe2b were transported to the site and the installation of the whole system took place, including the control and monitoring equipment.
4. Testing of TESSe2b: The solution was tested through the monitoring of critical parameters.
5. Technical and economical evaluation: The TESSe2b solution was evaluated.

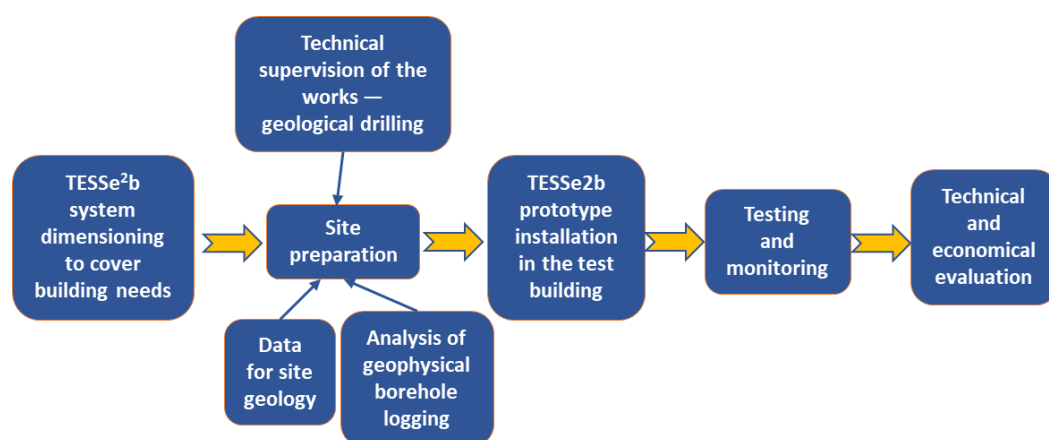


**Figure 1.** The steps followed for the research.

## 2.2. Dimensioning the TESse2b System Components for Demo Site in Austria

In this section, the dimensioning of the TESse2b system components for the demo site in Austria is presented.

### 2.2.1. The Area—Climatic Data

The demonstration site in Austria was located within the township of Kapfenberg/Styria, about 40 km north of Graz, the capital of Styria (see Figure 2). The selected house was located on the plot of a technical school, the HTL Kapfenberg.



**Figure 2.** Location of demonstration site in Austria [20].

Kapfenberg is located in a moderate continental climatic zone, where the long-term monthly mean temperature fluctuates between  $-2.3$  °C in winter (January) and  $17.8$  °C in summer (July) and the average annual temperature is  $8.1$  °C. The area is wind-poor, especially in winter, and therefore, prone to fog (frequent high-level fog). As a result, the duration of sunshine in winter is significantly affected and decreases in the valleys to values of less than 30 percent. The annual solar radiation can be quantified as ca.  $850$  kWh/m<sup>2</sup>. In summer, there is a significant rainfall maximum in relation to the year. Most of the precipitation falls in July, with an average of  $111$  mm, and the lowest amount occurs in February, with an average of  $32$  mm. The average annual rainfall is  $796$  mm. Rainfall fields often reach the area via the Hochschwab, a mountain in the main alpine ridge.

### 2.2.2. Geology of the Site—TRT Test

Based on measurements conducted during the drilling works for BHE development and up to  $75$  m, the first six meters consisted of deposited soil and quaternary gravels, followed by changing layers of paragneiss and quartzite down to a depth of  $31$  m [21]. Between  $31$  m and  $55$  m, the response of the NGR log reflected quartzite, with a fault zone between  $43$  and  $45$  m indicated by the change in the inclination of the borehole and fault gouge material with pyrite. The increase in inclination persisted to the bottom of the borehole. At the base of the pure quartzite, another fault zone occurred between  $55$  and  $58$  m, indicated both by the NGR and the DIEL log, and the cuttings as well. Below  $58$  m until the final depth of  $75$  m, another set of changing layers of paragneiss and quartzite appeared, which bore micaschists as well.

To define the actual thermal properties (the mean ground thermal conductivity and the borehole thermal resistance) of the underground and ground temperatures for the site, a thermal response test (TRT) was performed on one completed BHE in Austria (Figure 3) [21–23]. Water was circulated within the BHE and heated at a constant power load. The temperatures at the inlet and outlet were recorded over a period between 50 and 72 h. Based on the temperature difference between two logarithmic decades, the thermal conductivity was calculated. The heating of the testing circuit with constant power was ensured by using electric heaters and a constant voltage power supply, whereas the fluid flow was kept constant by the variable speed (inverter)-type circulation pump used. The temperature spikes observed after the initiation of the heat input were caused by the difference between the BHE temperature and the temperature of the buffer used to house the heating element. This response disturbance is well known when performing TRT tests, and the region before stabilization (before 5000 s) was not taken into consideration when calculating the ground conductivity.

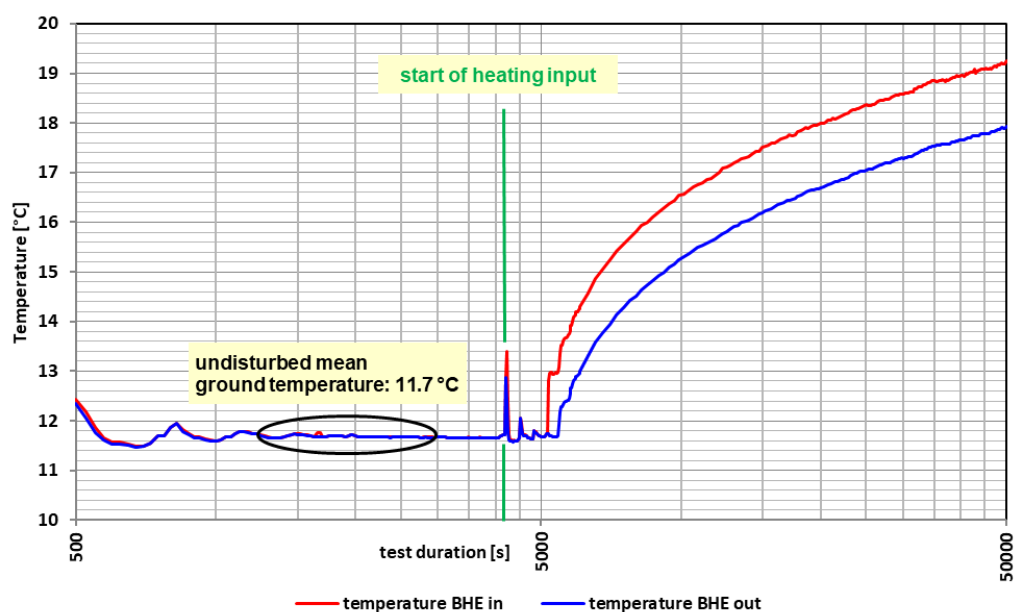


**Figure 3.** Determination of the undisturbed mean underground temperature [21].

As a result, the mean thermal conductivity for a BHE with a length of 75 m was determined at 2.22 W/(m·K) using the following equation:

$$l = \frac{2.302 \cdot Q}{4 \cdot \pi \cdot h \cdot \Delta T}$$

where:

$l$  = thermal conductivity [W/(m·K)];  $Q$  = constant heat delivery [W];  $h$  = height (=length of BHE) [m]; and  $\Delta T$  = temperature difference [K].

An additional value that was determined was the thermal borehole resistance, which describes the thermal resistance of the grouting material and is an indicator of the thermal connection between BHE and the ground, and of the quality of the BHE itself. A value of 0.100 (m·K)/W was determined for the Kapfenberg site. The mean ground temperature measured using TRT was 11.7 °C.

### 2.2.3. Building Characteristics

The house was constructed in 2003 with a wall thickness of 38 cm, and consisted of solid bricks [13,20]. Thermal insulation of the whole building was implemented in 2010, adding 16 cm of EPS at the base and 18 cm of EPS in the walls. The roof was isolated with 14 cm of mineral rock wool. The house contained two independent residential units (Unit 1 and Unit 2) with a total area of 202 m<sup>2</sup> (Figure 4), while a cellar was located in the

southern part of the building. The heating design was implemented for the whole building. Before thermal insulation, an oil burner with a capacity of 33–37 kW and that also provided the domestic hot water in a 400 L tank was run to cover the demand. As the system was not changed after the retrofitting, the heating of the building was uneconomical. The installed radiators required an ingoing temperature of 65 °C. The annual oil consumption was around 4000 L of oil, which can be converted to 40,000 kWh/year.

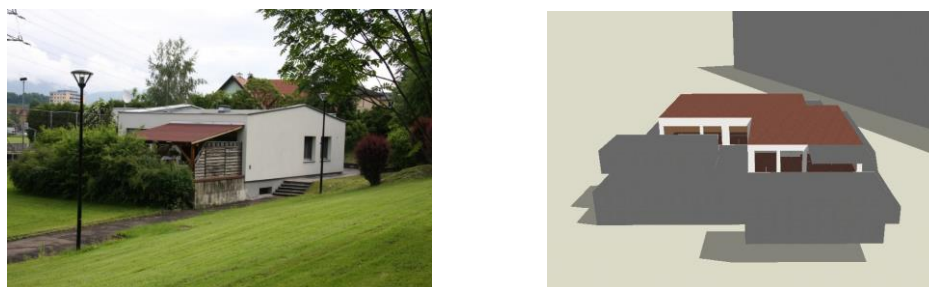


**Figure 4.** External view of the building (left) and geometric model (right) [20].

#### 2.2.4. Dimensioning the TESSe2b System—Installation in the Building

Considering the house usage characteristics, the energy requirements of the building were calculated using the Design Builder V4.0 software [19] in order to dimension the TESSe2b system for heating and DHW and evaluate their performance. Climate data for Graz, Austria, provided by Design Builder, were used, while measurements recorded by the weather station that was installed at the demo site were used for validation. The following assumptions were considered: only heating mode, no cooling mode; heating period: October to May; indoor temperature: 22 °C; heating distribution system: heating floor (Unit 1) and radiators (Unit 2); utilization schedules of heating: depending on the room/24 h during the heating period; DHW: 4 persons, 160 lt per day; 45 °C; estimated usage profile; solar collectors: vacuum tubes; and available solar energy priorities: 1st—DHW, 2nd—heating needs and charging of HTES tank.

For the heating mode, the capacity was 14.4 kW, corresponding to 75.14 W/m<sup>2</sup>, and the annual need was 18,537.1 kWh. For the cooling mode, the capacity was 4.7 kW and the annual need was 2891 kWh. Considering the low cooling needs, it was decided that the demo site would be cooled with free-cooling. Based on the results obtained in the dynamic simulation in Design Builder, an analysis of the TESSe2b system was performed to optimize the number of tanks and solar collectors. Due to area restrictions, the solar collectors' area was halved to approx. 13.6 m<sup>2</sup>.

The heating and DHW system in Austria comprised the following parts:

- Solar collectors, serving either the HTES or the DHW tanks.
- Geothermal installation with: heat pump and 4 BHEs (2 with and 2 without PCM) with a single U-tube of 40 × 3.7 mm, 75 m each, and 300 m total. The drillings for the BHEs encountered alternating layers of paragneiss and quartzite as the bedrock, after six meters of deposited soil and quaternary gravels. None of the rocks were water-bearing. The connection tubes from the BHEs into the house were installed in a pattern that ensured comparable lengths between the BHEs further from and nearer to the house [20].
- HTES tanks for heating.
- DHW supply with:
  - DHW TES tank (charged either by the solar collectors or the heat pump);
  - DHW backup;
  - DHW circulation circuit.
- Buffer tank: working as hydraulic separator between the respective loops and serving the heating circuits of both residential units.
- TESSe2b control and monitoring system.

The TESse2b hydraulic scheme for the demo building in Austria is shown in Figure 5, as it was customized [20].

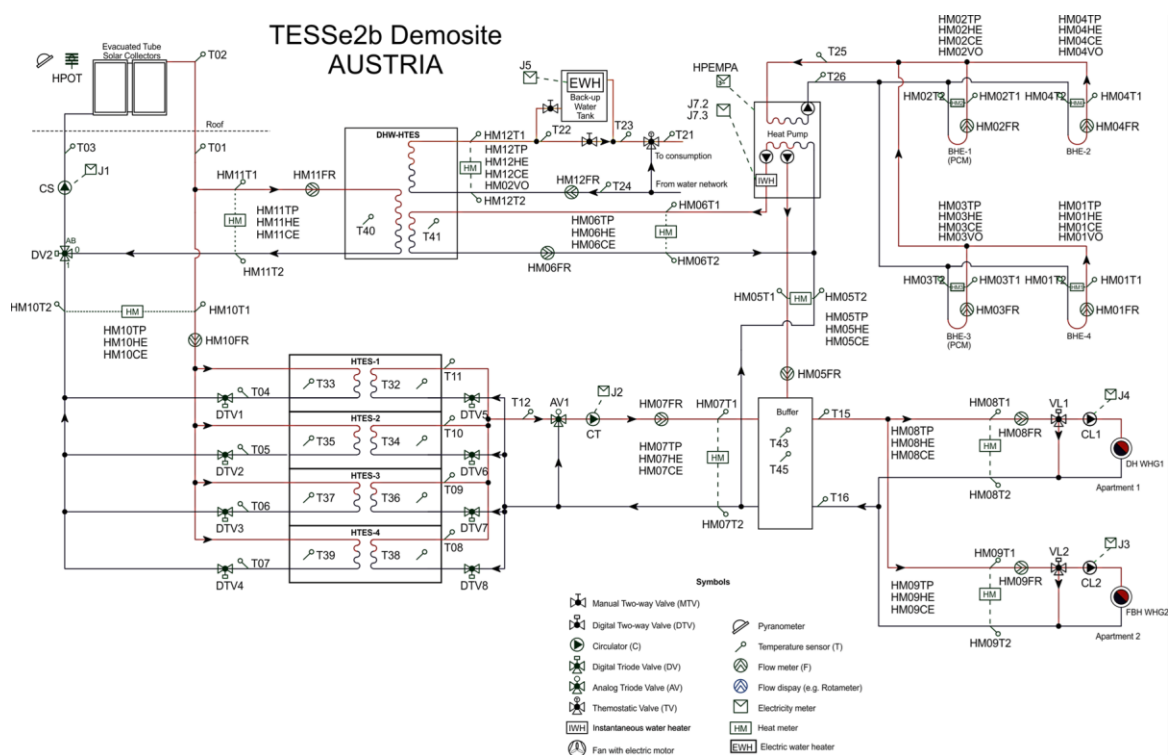


**Figure 5.** Hydraulic scheme for TESse2b in Austrian demo site [20].

**Solar collectors:** The installed type of solar collector was VITOSOL<sup>®</sup> 300-TM (manufactured by Viessmann<sup>®</sup>, Allendorf, Germany), a highly efficient solar collector with vacuum tubes. The integrated heat protection automatically shut off the collector and ensured the integrity of the collectors during high solar radiation. Solar collectors with a total absorber area of 13.63 m<sup>2</sup> and a total gross area of 20.84 m<sup>2</sup> were installed. This quantity was the highest possible to be installed, as more collectors could affect the static integrity of the roof.

**TES tanks:** Three tanks filled with organic PCM A44 [24] for heating (HTES tanks) and one tank filled with PCM A53 [24] for the domestic hot water supply (DHW TES tank) were installed in the room originally containing the oil tank (Figure 6). The PCM tanks were designed and constructed by the research team [15–17,25]. The tank assembly consisted of plastic molded containers, in which the fin and tube HE were immersed. The HE had two separate hydraulic circuits, one connected to the solar hydraulic network and the other connected to the building's heating/DHW network. The space inside the plastic containers (surrounding the fins of the HE) was filled with the PCM. The outer surface and top lid of the plastic tanks was insulated with polyurethane insulating foam, and the overall construction was enclosed in a sheet metal cover for mechanical protection. The PCM was inserted into the tanks after construction in liquid form. To liquify the PCM, temporary boiling water baths were employed. The PCM in the tanks was at atmospheric pressure, and proper venting was installed. The PCM used was not volatile and was operated well below its evaporating point.



**Figure 6.** TES tanks in Austria [20].

**Geothermal installation:** Four BHEs with an individual length of 75 m (300 m in total) were drilled for the geothermal energy supply of the house, two of them with and two without PCM [21]. Two of them were completed as single-U-tube BHEs with a diameter of  $40 \times 3.7$  mm; two BHEs were completed as double-U-tube BHEs with the same diameter; and one circuit was filled with the PCM. The BHEs were drilled in a rectangular configuration, as shown in Figure 7, with a distance of seven meters between them. For the installation of the pipes, the layout was chosen to ensure a comparable length between the PCM-BHEs and the common ones.



**Figure 7.** Left: procedure for injection of PCM into BHEs; top right: photo of a completed BHE; bottom right: section of a BHE. 1—ground, 2—borehole (space for grout), 3—BHE tubes, 4—injection tube [20].

A mortar-mixing pump was used for the grouting, and the grouting pipes were set on the bottom of the boreholes. For optimal heat transfer between the ground and the BHEs, a thermally enhanced grout especially for BHEs with a thermal conductivity of  $2 \text{ W}/(\text{m}\cdot\text{K})$  was used (Röfix<sup>®</sup> CC856, Röfix, Rothis, Austria). The PCM selected to fill the BHEs had a nominal phase-change temperature of  $9 \text{ }^\circ\text{C}$ , and its phase-change region was measured (as part of the project requirements) to be  $5\text{--}13 \text{ }^\circ\text{C}$ , covering the entire operating temperature region of the BHE's effective length (5–75 m), given that the normal geothermal gradient in the area was  $0.033 \text{ }^\circ\text{C}/\text{m}$  and the undisturbed mean BHE temperature was measured to

be 11.7 °C during the TRT tests. After completion, a pressure test was performed at each BHE. The connection tubes from the BHEs into the house were installed in a pattern that ensured comparable lengths between the BHEs further from and nearer to the house. Also, the tubes for the inlet and outlet were led separately for every respective BHE into the house to enable the installation of one heat meter for every single BHE. By this means, the parameters of temperature (for the inlet and outlet), flow, and energy could be monitored for each heat exchanger (Figure 8).



**Figure 8.** BHE inlets and outlets after the installation of the heat meters [20].

A Viessmann® brine–water heat pump with a compliant-scroll compressor (model: Vitocal 301.B13, Viessmann, Allendorf, Germany) was installed (Figure 9), with a rated heating output of 13.0 kW, a power consumption of 2.6 kW, a COP of 5.0, and a max. outflow temperature of 65 °C.



**Figure 9.** Heat pump installed at Austria demo site [20].

**Back-up system:** To ensure a sufficient DHW supply in case of problems with the DHW TES tank, a backup system was installed that consisted of a common 150 lt hot water tank heated by an electric resistance.

**Terminal units:** In Unit 1, the old radiators were replaced by new radiators with an increased heating surface. In Unit 2, larger renovation works were performed, as massive ground heaving had caused severe floor damage, which made it necessary to replace the entire floor in this unit. This opened up the opportunity to install a floor-heating system and to completely retrofit the layout for the unit.

**Auxiliary devices:** Grundfos® (Bjerringbro, Denmark) high-efficiency circulators for the heating units, immersion temperature sensors and 3-way valves, Kamstrup® MULTICAL 603 heat meters (Kamstrup, Roswell, GA, USA), Kamstrup® ULTRAFLOW 54 ultrasonic flow meters (Kamstrup, Roswell, GA, USA), and a hot water circulation circuit were

used to ensure an instantaneous hot water supply whenever a tap was opened. Finally, a Davis® Vantage Pro 2 Plus Wireless (Davis Instruments, Hayward, CA, USA) weather station was installed to monitor the weather in the area of the building.

Control and monitoring system: The control and monitoring system comprised the TESSe2b controller and the components shown in Table 1.

**Table 1.** Components of TESSe2b control and monitoring system.

Type	Description
Monitoring system	Collects and stores all data needed for the monitoring and evaluation of the performance of the TESSe2b system on a remote data server, where they are stored in a structured database for later access.
Actuators	Two-way and three-way electronic control valves: Belimo ball valves, R2025/R3025, with electronic actuators, LR24A. High-efficiency variable-speed circulating pumps with PWM speed control: Grundfos Alpha Solar (Grundfos, Bjerringbro, Denmark) and Alpha2 (Grundfos, Bjerringbro, Denmark) heat pump (operating mode and temperature set points).
Sensors	Temperature sensors: Siemens QAE2112.015 Pt-1000 (Siemens, Munich, Germany), 4-wire, $\pm 0.5$ K accuracy in the required measuring range, time constant of 3 s. Room temperature and humidity sensors: SYsnsTH001 $\pm 0.5$ K temperature accuracy, $\pm 0.3\%$ relative humidity accuracy.
Meters	Heat meters: Kampstrup MULTICAL® 603 and MULTICAL® 6M2 with a typical accuracy of $E_C \pm (0.5 + 2/\Delta\theta) \%$ and $E_T \pm (0.4 + 5/\Delta\theta) \%$ according to Standard EN 1434-1. Electricity meters: Schneider iEM3000; active power accuracy Class 1 conforming to IEC 62053-21 and IEC 61557-12; reactive power accuracy Class B conforming to EN 50470-3.
Data communication protocol converters	They were used to convert data formats between the data communication protocols control area network (CAN), MODBUS RTU, and M-BUS, as shown in Figure 10.

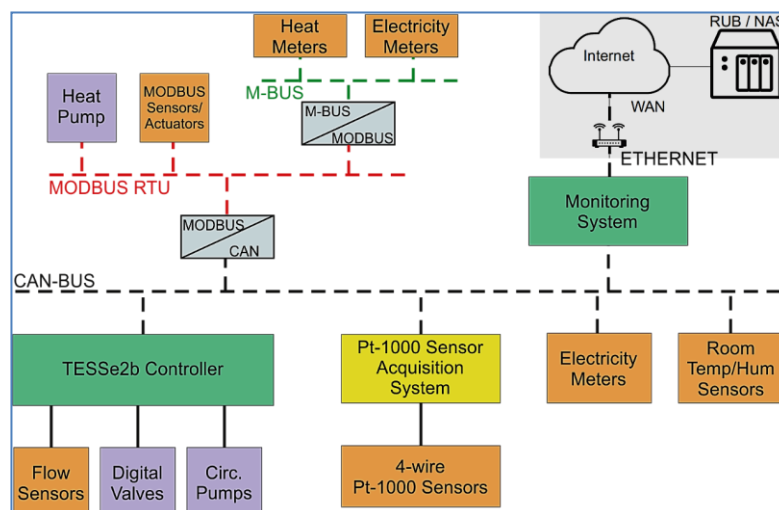


**Figure 10.** Diagram of TESSe2b control and monitoring system [18,20].

Data communication was achieved between the TESSe2b controller, the monitoring system, the heat pump, and all the sensors and actuators in the hydraulic installation. The monitoring system collected the measured data and the status of each device in the system, which were uploaded through an ethernet connection in a structured SQL

database using network-attached storage (NAS). Access to real-time and historical data was provided through a password-protected website (Figure 10) [18,20]. The database and the website could also be used to remotely control the system, for example, for setting system parameters or for selecting user preferences such as daily time schedules and operating modes.

The TESSe2b system operation should cover the heating needs of the building (through the use of solar and geothermal energy) and domestic hot water. Other operations of the system included the storage of solar and geothermal energy for heating using TES tanks and the safe operation and protection of the system components. The inlet and outlet temperature of the heating/cooling devices was controlled by the TESSe2b controller, and the flow and temperature of the heat transfer fluid in the load loop was regulated so as to ensure that the appropriate amount of energy was efficiently supplied to the house. Furthermore, the TESSe2b controller ensured that the desired DHW temperature was provided at all times to meet the needs for DHW consumption. The controller communicated with the GSHP through a CAN-Bus/MODBUS RTU converter and read the operating status information of the GSHP. When needed, it gave commands to change the operation of the GSHP between DHW, heating, and cooling, and it gave commands to change the outlet temperature of the GSHP. The controller ensured that the operating temperatures of the HTES tanks were sustained within the safety limits of the PCM and the tank in order to extend their lifetime. It also performed other safety functions, e.g., a safety operation in case of a component failure or during extreme weather conditions, and heat dissipation in case of excess solar energy.

The TESSe2b system can be installed both in new residential buildings and in existing buildings without the need to replace the heating devices. This is possible because the TESSe2b controller is independent of the building installation. Decentralized control devices and thermostats, which are not an integral part of the TESSe2b system, as they depend on the type of the heating devices of the building, are responsible for the temperature control of individual rooms or zones. Sensor signals and user inputs are evaluated by the central TESSe2b controller, which applies an algorithm to select and apply the best operation modes for the system depending on the load demand, the solar availability, the state of charge of the storage tanks, and the overall system efficiency (Figure 11).



**Figure 11.** Control cabinet in Austria [20].

### 2.3. Use of PCM in the BHEs

When GSHP operates in heating mode, a decrease in the temperature of the heat transfer fluid within the BHE will take place. Due to the low thermal diffusivity of the ground, a much slower ground thermal response than the heat pump requirements takes place, which causes thermal waves to transmit into the ground through the BHEs. This

results in a lower coefficient of performance (COP) of the GSHP. The addition of PCMs to the grouting suspension is considered an effective means to store thermal energy in the BHEs, thus improving the effectiveness of the BHEs. By this measure, the generated thermal wave should be smoothed, thus increasing the SPF (seasonal performance factor) of the GHSP system, as this applies to the heating and cooling modes.

According to the technical recommendations that are applied in most of the licensing procedures in Austria, the lower limit for the average fluid temperature is  $-1.5\text{ }^{\circ}\text{C}$ . In view of the expected low temperature, the selected PCM should provide energy in a temperature range between the low values and the temperatures of the surrounding soil, so that the PCM can support the system by stabilizing the temperatures at a higher level during the operation of the heat pump. During the shut-down period, the PCMs will be recharged by the natural heat flow. As the system in Austria was used mainly for heating, a PCM with a phase transition temperature ranging 3 degrees below the estimated medium ground temperature ( $11.7\text{ }^{\circ}\text{C}$ ) was chosen, namely the commercial product A9, which is a naturally derived blend of alkanes [24].

Since the PCMs were used in boreholes, and therefore, they were in contact with the environment, they were encapsulated in order to prevent any interaction between the PCM and the grout, ground, or groundwater. The methods of encapsulation that were tested for the TESSe2b system included microencapsulation, silica powder, and macroencapsulation. Macroencapsulation using double U-tubes was favored, as this installation method is widely used in the market and it implements the lowest environmental risk while being cost-effective. The basic design of the PCM-BHE consisted of a common double U-tube where one of the circuits was filled with the PCM instead of the heat carrier fluid. The BHEs were filled with water when inserted into the borehole to ease the operation. To evacuate the water, the BHE pipe was connected to a compressor and the water was blown out with a pressure of up to 12 bar. After that, the PCM (A9) was easily poured into the tubes, although the outside temperature was close to the PCM phase-change temperature. The two BHEs were filled with a total amount of 125 l each, for 250 l in total.

### 3. Evaluation Results for TESSe2b System Performance—Discussion

#### 3.1. Methodology

An evaluation was conducted at various levels, as explained by the following. Initially, the TESSe2b solution was compared with the most common conventional system used for heating and domestic hot water in Austria, which is the boiler and burner system using heating oil. The monitoring results for the heating mode were used for the TESSe2b calculations. The climatic and meteorological data of the area, the building cell's technical characteristics, and the typical building use were applied to calculate the energy consumption of TESSe2b for the case of the conventional system with Design Builder [19]. For an assessment of the TESSe2b system in comparison with the conventional system, proper indicators were calculated: the annual energy savings, the reduction in the operational cost, and the simple pay-back period.

The TESSe2b system's effectiveness at the Austria demo site was further assessed by considering two quantities: (i) SPF3, which is the system efficiency and includes the electricity consumption of the GSHP, the circulator to the BHEs, and the buffer tank and instantaneous water heater (IWH) that are all included in the GSHP, and (ii) SPF4, which is the system's efficiency and includes the electricity consumption of the GSHP, the circulator to the BHEs, the buffer tank and IWH that are all included in the GSHP, and finally, the circulators CL1 and CL2 (Figure 5) to the house distribution system (Unit 1 and Unit 2).

In conclusion, the storage system performance of a TESSe2b system was evaluated while also taking into account the required volume to achieve the same results while using water as the storage medium.

### 3.2. Evaluation of TESSe2b in Comparison with the Conventional System

A boiler and burner system, using heating oil with 24.9 kW for heating and DHW, was used. The following assumptions were considered: the temperature of the radiators at the inlet is 80 °C, while the outlet temperature of the boiler is 80 °C. The domestic hot water tank volume is 160 lt, and its outlet temperature is 50 °C. The min. temperature of fresh water is 7 °C and the max. temperature of fresh water is 13 °C. The calculation of the indicators requires the energy heating needs to be converted to primary energy using conversion factors (Table 2). In parallel, the annual reduction in CO<sub>2</sub> emissions was calculated. Graz weather data from the Design Builder database were used. The data were compared with those obtained by the weather station installed on the demo site, showing a good agreement for an entire year.

**Table 2.** Energy source conversion factors.

Energy Source	Primary Energy Conversion Factor	Emissions TCO <sub>2</sub> /MWh
Oil	1.230	0.267
Electrical Energy	1.910	0.209

The results show that, for the conventional system, the oil consumption for heating and DHW was 25,421.7 kWh and the equivalent primary energy for heating and DHW was 31,268.6 kWh. For the TESSe2b system, the electricity consumption for heating and DHW was 2568.7 kWh and the equivalent primary energy for heating and DHW was 4906.3 kWh.

The annual amount of primary energy savings was 84.31%, which led to annual emission reductions of 6.795 TCO<sub>2</sub> and an annual savings in operational and maintenance costs of 79.71%. Additionally, the simple pay-back period for newly installed systems was 8.7, which is less than 10 years.

The total cost for the TESSe2b system was EUR 27,600, which included the various component costs, such as the heat pump (EUR 13,000), solar collectors (EUR 7000), TES tanks (EUR 4500), monitoring and control system (EUR 1350), and auxiliary devices (EUR 1750). The installation cost of the conventional system (oil boiler and burner and the auxiliary devices) was EUR 8950. It has to be mentioned that the costs of the terminal units and the DHW heater were exempted from the economic analysis, since the two systems, the TESSe2b and the conventional one, have both the above-mentioned costs. It is anticipated that the associated costs will decrease during the TESSe2b commercialization phase.

The calculated SPF3 are given in Table 3. According to the SPF results, it was evident that, during the heating period in Austria (May 2019), the SPF3 of 3.4—which comprised the electricity consumption of the compressor and circulators to the BHEs and the buffer tank, as well as the IWH—showed a very good performance for the entire system, and this was also expressed by SPF4, which contained additional circulators to the distribution system of the house. Furthermore, the SPF4 of 3.36 showed a slight difference in relation to SPF3, which means that the electricity consumption of the circulators for the distribution system of the house was not significant.

**Table 3.** SPFs from TESSe2b implementation in Austria.

	SPF3	SPF4
May	3.40	3.36
June	12.50	11.60
July	6.37	5.90
August	4.71	4.35

During June 2019, the TESSe2b system operated in heating mode for a very short period and also produced DHW, which was the reason for the very high values of SPF3 and SPF4. On the other hand, only DHW production by TESSe2b during July and August 2019 led to

a high SPF3 and SPF4, with higher values of SPFs in July, where the DHW production was higher due to a higher solar fraction.

### 3.3. Storage System Performance

Using the operational profiles to calculate the storage system performance, an hourly energy analysis of heating and DHW production was performed. In Table 4, it is shown that the analysis results of the TES tanks for heating and DHW in relation to the solar contribution and the energy needs shifted from day (higher electricity tariffs) to night (lower electricity tariffs). The results were obtained without any influence from the self-learning control system and without the influence of the use of PCM in the boreholes, which may have contributed to the increase in the system performance.

**Table 4.** Results of hourly energy analysis of heating and DHW production.

Solar collectors	4
Solar fraction heating	7.0%
Solar fraction heating + DHW	15.8%
Heating needs shifted day to night (total solar)	41.6%

In Figure 12, it is possible to observe the results from when the system operated for three days in March (heating mode). The heating needs in those three days were satisfied by the available solar energy through the TES tanks.

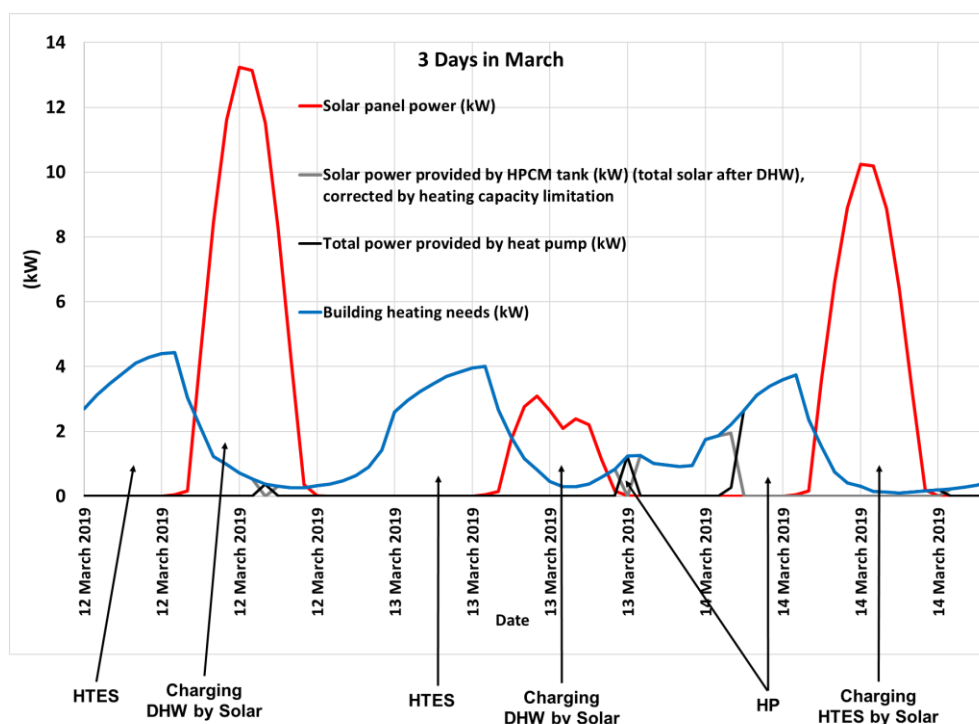


**Figure 12.** Results from system operation for three days in March (heating mode).

The main characteristics of the four TES tanks were as follows: a total amount of energy stored (for heating) of 29.2 kWh and an average TES capacity (heating) of 18 kW. The characteristics of the DHW TES tank were as follows: a total amount of energy stored (DHW) of 6.2 kWh and a supply water temperature of 40–50 °C.

The heating capacity was higher than that of the installed capacity of the respective heat pump. This means that, as long as the TES tanks had stored energy, they were able to cover all the needs, even at peak times, without any help from the heat pump. The total volume

of the DHW and the HTES PCM storage was  $0.8 \text{ m}^3$ , and based on the calculations with Design Builder, the necessary volume of water energy storage to produce the same solar fraction as the PCM tanks, for heating and DHW, using the same area of solar collectors, was  $3.5 \text{ m}^3$ . The advantage of the necessary limited space with PCM storage instead of water storage is obvious.

In Figure 13, the building heat consumption, calculated using Design Builder V4.0 and as measured by monitoring for a week in October, are shown. The energy delivered by the TESSe2b system to the building that week was 360.8 kWh, and Design Builder's predicted value was 331.0 kWh, representing a difference of 8.2%, which shows a proper agreement between Design Builder and demo site monitoring. The monitoring data showed the influence of the control system, where the slight variations have to do with the dead band set for the temperature control. Another reason for the difference between the evolutions of the two lines has to do with the influence of the thermal inertia of water within the distribution system. Considering those differences and their evolutions in the graph, as well as the above, it was considered that the simulation adequately represented the actual functioning of the building, allowing conclusions to be drawn regarding the performance of the conventional system and the TESSe2b system.

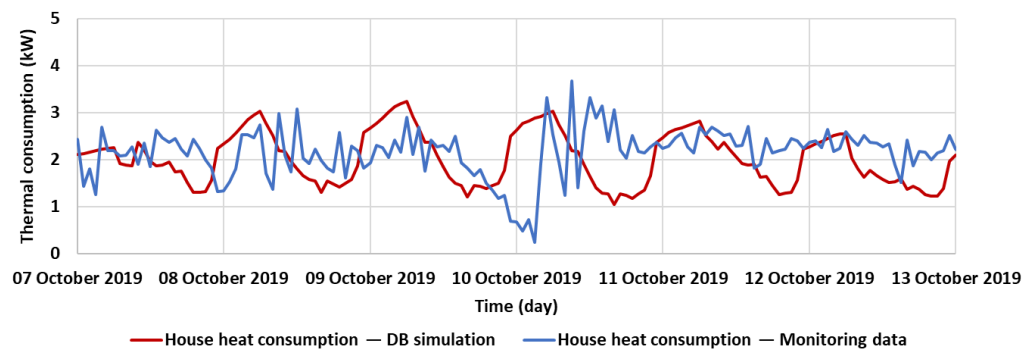


**Figure 13.** The heat consumption profile of the house—a comparison between the simulation and monitoring data.

Figures 14–19 show the TESSe2b system's performance in the Austrian demo site over two days during the heating season. A day with less available solar energy, 9 October (Figures 14–16), and a sunny day at the beginning of the heating season, 15 September (Figures 17–19), are shown. In Figure 17, the horizontal solar radiation intensity is shown, as measured by the weather station and the charging rate of both thermal energy storage tanks (HTES and DHW TES) through the solar collectors. The solar system started to charge the DHW TES tank, which was a priority of the control system. The charging rate was highly dependent on the solar radiation intensity, as expected, and it achieved a maximum value of 8 kW for the DHW TES tank and approximately 10 kW for the HTES tanks. The charging rate values were in the range of the values recorded in the laboratory [15,16]. In Figure 18, the heat transfer rate between the buffer tank and the other components of the heating system is shown. The monitoring data shows that the HTES tanks were exclusively charged by the solar collectors, and a significant part of the heat provided to the house came from the solar collectors through the HTES tanks. The significant contribution of the HP to the heating system was after the HTES tanks were discharged between 3:00 and 4:00, and between 7:00 and 7:30.

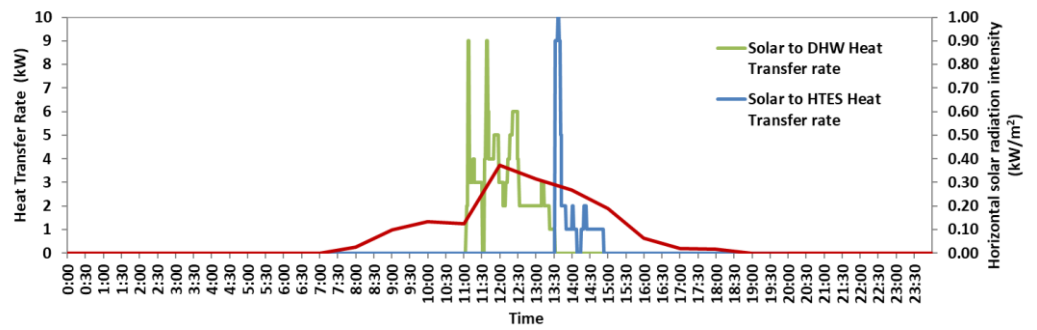


**Figure 14.** The heat transfer rate from the solar collectors to the DHW TES and HTES tanks and the solar radiation intensity over a horizontal surface on 9 October 2019.

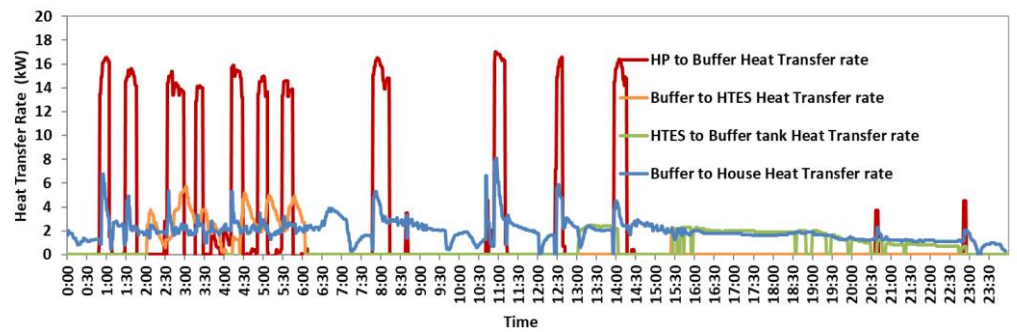


**Figure 15.** The heat transfer rate between the buffer tank and the HP, the HTES tank, and the house's heating system on 9 October 2019.

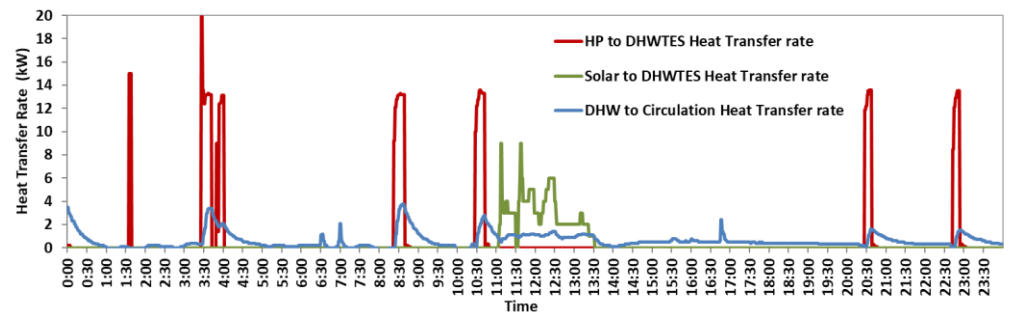


**Figure 16.** The heat transfer rate from the solar collectors and the HP to the DHWTES tank and from the DHWTES tank to the house's DHW circulation system on 9 October 2019.

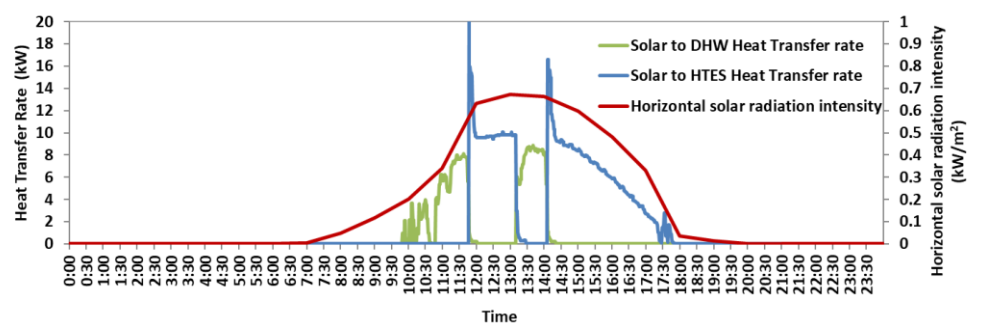


**Figure 17.** The heat transfer rate from the solar collectors to the DHWTES and HTES tanks and the solar radiation intensity over a horizontal surface on 15 September 2019.

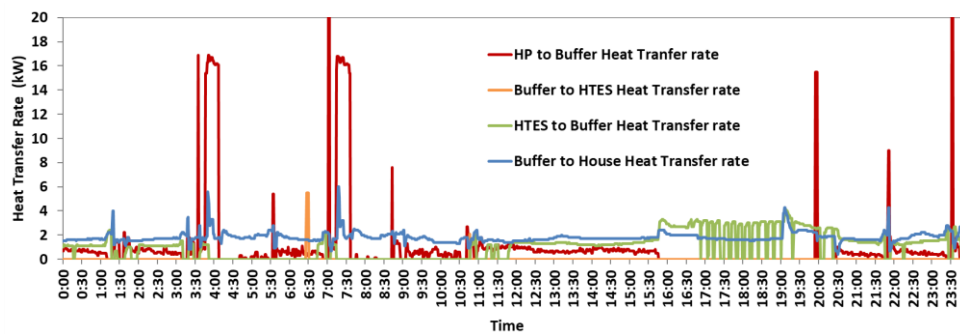


**Figure 18.** The heat transfer rate between the buffer tank and the HP, the HTES tank, and the house's heating system on 15 September 2019.

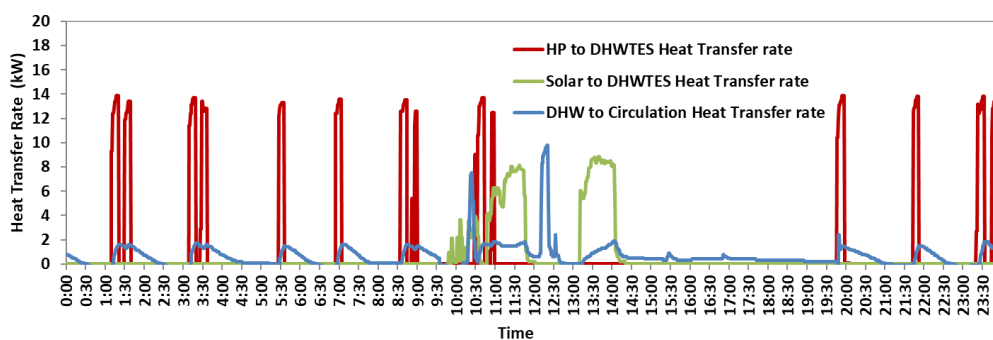


**Figure 19.** The heat transfer rate from the solar collectors and the HP to the DHWTES tank and from the DHWTES tank to the house's DHW circulation system on 15 September 2019.

Considering the DHW, the backup system never worked, and the DHW was fully provided for by the TESSe2b system. The monitoring data presented in Figure 19 indicate that, between 11:00 and almost 20:00, the DHW provided to the circulation system was heated by the solar collectors through the DHW TES tank; outside of this period, the DHW TES tank was charged by the HP. The discharging rate was in the range of values recorded in the laboratory [15,16]. The differences were due to the differences in the operation conditions.

On October 9th, the results presented in Figure 16 show, qualitatively, a similar behavior to September 15 (Figure 19); the solar system started to charge the DHW TES tank, and after that, it charged the HTES tanks. Nevertheless, the charging rate and the total thermal energy stored were smaller due to the lower solar radiation. Regarding the heating system, in Figure 16, it is indicated that, during the night between 2:00 and 6:00, the HP was used to provide heat to the house and to charge the HTES tanks. The time operation of the HP was higher during the night at the low-electricity-tariff period. The energy stored in the HTES tanks was used to heat the house between 12:00 and 23:00 h. Concerning the DHW system, the HP was only used during short periods before 11:00 and after 20:30; between 11:00 and 20:30, the DHW was provided by the solar system.

The results presented above clearly illustrate the advantages of the TESSe2b solution comparatively to the conventional system. Thermal storage extends the capacity of providing solar thermal energy to a house beyond the solar hours in a day, and also gives flexibility to the heating system, concentrating the heat pump operations during the low-electricity-tariff periods.

#### 4. Conclusions

In this work, the effectiveness of an innovative thermal energy storage application installed in a building in Austria, where heating needs prevail, was assessed, and the following conclusions were reached:

- The demonstrated system achieved a reduced primary energy consumption, decreased maintenance costs, and an overall economical operation. The overall system installation cost increased, but was offset by the efficient operation of the system, thus resulting in an acceptable pay-back period.
- The percentage of annual primary energy savings from the TESSe2b system in relation to the conventional system in Austria (boiler and oil burner for heating and DHW) was 84.31%, and the percentage of annual savings in operational and maintenance costs was 79.71%. Additionally, the simple pay-back period for newly installed systems was 8.7, which is less than 10 years. This is a promising technology, since the simple pay-back time is acceptable and it can be significantly reduced during its commercialization phase.
- The TES tanks exhibited an energy capacity that was capable of supplying the heating and DHW needs of the building, even during high-demand times; thus, the heat pump was turned off during hours when the PCM tanks supplied the load.
- The results presented above clearly illustrate the advantages of the TESSe2b solution comparatively to the conventional system. The thermal storage solution not only increases the use of solar thermal energy by extending the capacity of providing solar thermal energy to the house beyond a day's solar hours, but it also gives flexibility to the heating system, concentrating the heat pump operation during the low-electricity-tariff periods.
- The overall system was designed to be compact in order to be installed in a conventional mechanical room. The overall system volume for the presented demo site was 1.55 m<sup>3</sup>.

**Author Contributions:** Conceptualization, L.C., M.G.V., C.K. and C.S.; methodology, L.C., M.G.V., C.K., C.S., J.G., P.T. and M.K.K.; software, P.T., C.S. and A.R.; validation, all authors; formal analysis, M.K.K., P.T., J.K., A.R. and A.B.; investigation, M.K.K. and J.K.; writing—original draft preparation, M.K.K. and J.K.; writing—review and editing, M.K.K., J.K. and L.C.; supervision, L.C. and M.G.V.; project administration, L.C.; funding acquisition, M.G.V. and L.C. All authors have read and agreed to the published version of the manuscript.

**Funding:** The TESSe2b project received funding from the European Union's Horizon 2020 Research and Innovation Programme under the grant agreement number 680555.

**Data Availability Statement:** Data are contained within the article.

**Conflicts of Interest:** Authors Heiko Gaich and Johan Goldbrunner were employed by Geoteam Technisches Buro fur Hydrogeologie, Geothermie und Umwelt GMBH. The remaining authors declare that the research was conducted in the absence of any commercial or financial relationships that could be construed as a potential conflict of interest. The funder was not involved in the study design, collection, analysis, interpretation of data, the writing of this article or the decision to submit it for publication. This article reflects only the authors' views, and the commission is not responsible for any use that may be made of the information it contains.

## References

1. The European Green Deal. Available online: [https://commission.europa.eu/strategy-and-policy/priorities-2019-2024/european-green-deal\\_en](https://commission.europa.eu/strategy-and-policy/priorities-2019-2024/european-green-deal_en) (accessed on 16 August 2023).
2. The Paris Agreement Publication. Available online: <https://unfccc.int/documents/184656> (accessed on 18 August 2023).
3. BPIE (Buildings Performance Institute Europe). *Ready for Carbon Neutral by 2050? Assessing Ambition Levels in New Building Standards Across the EU*; BPIE: Brussels, Belgium, 2022; Available online: [https://www.bpie.eu/wp-content/uploads/2021/12/BPIE\\_Assessing-NZEB-ambition-levels-across-the-EU\\_HD.pdf](https://www.bpie.eu/wp-content/uploads/2021/12/BPIE_Assessing-NZEB-ambition-levels-across-the-EU_HD.pdf) (accessed on 18 August 2023).
4. Al-Sakkaf, A.; Zayed, T.; Bagchi, A. A Sustainability Based Framework for Evaluating the Heritage Buildings. *Int. J. Energy Optim. Eng.* **2020**, *9*, 49–73. [CrossRef]
5. Skandalos, N.; Karamanis, D. An optimization approach to photovoltaic building integration towards low energy buildings in different climate zones. *Appl. Energy* **2021**, *295*, 117017. [CrossRef]
6. Yao, S.; Yang, L.; Shi, S.; Zhou, Y.; Long, M.; Zhang, W.; Cai, S.; Huang, C.; Liu, T.; Zou, B. A Two-in-One Annealing Enables Dopant Free Block Copolymer Based Organic Solar Cells with over 16% Efficiency. *Chin. J. Chem.* **2023**, *41*, 672–678. [CrossRef]

7. Liu, T.; Zhou, K.; Ma, R.; Zhang, L.; Huang, C.; Luo, Z.; Zhu, H.; Yao, S.; Yang, C.; Zou, B.; et al. Multifunctional all-polymer photovoltaic blend with simultaneously improved efficiency (18.04%), stability and mechanical durability. *Aggregate* **2022**, *4*, e308. [[CrossRef](#)]
8. European Association for Storage of Energy and European Energy Research Alliance. *Joint EASE/EERA Recommendations for a European Energy Storage Technology Development Roadmap towards 2030*; Martens, D., Ed.; EASE/EERA: Brussels, Belgium, 2013.
9. Pandey, A.; Hossain, M.; Tyagi, V.; Rahim, N.A.; Selvaraj, J.A.; Sari, A. Novel approaches and recent developments on potential applications of phase change materials in solar energy. *Renew. Sustain. Energy Rev.* **2018**, *82*, 281–323. [[CrossRef](#)]
10. Faraj, K.; Khaled, M.; Faraj, J.; Hachem, F.; Castelain, C. A review on phase change materials for thermal energy storage in buildings: Heating and hybrid applications. *J. Energy Storage* **2020**, *33*, 101913. [[CrossRef](#)]
11. Yang, W.; Xu, R.; Yang, B.; Yang, J. Experimental and numerical investigations on the thermal performance of a borehole ground heat exchanger with PCM backfill. *Energy* **2019**, *174*, 216–235. [[CrossRef](#)]
12. Koçak, B.; Fernandez, A.I.; Paksoy, H. Review on sensible thermal energy storage for industrial solar applications and sustainability aspects. *Sol. Energy* **2020**, *209*, 135–169. [[CrossRef](#)]
13. TESSe2b—The Smart Energy Storage. Available online: <https://cordis.europa.eu/project/id/680555> (accessed on 5 November 2022).
14. Soares, N.; Costa, J.J.; Gaspar, A.R.; Santos, P. Review of passive PCM latent heat thermal energy storage systems towards buildings' energy efficiency. *Energy Build.* **2013**, *59*, 82–103. [[CrossRef](#)]
15. Dogkas, G.; Konstantaras, J.; Koukou, M.K.; Vrachopoulos, M.G.; Pagkalos, C.; Stathopoulos, V.N.; Pandis, P.K.; Lymperis, K.; Coelho, L.; Rebola, A. Development and experimental testing of a compact thermal energy storage tank using paraffin targeting domestic hot water production needs. *Therm. Sci. Eng. Prog.* **2020**, *19*, 100573. [[CrossRef](#)]
16. Koukou, M.K.; Dogkas, G.; Vrachopoulos, M.G.; Konstantaras, J.; Pagkalos, C.; Stathopoulos, V.N.; Pandis, P.K.; Lymperis, K.; Coelho, L.; Rebola, A. Experimental assessment of a full scale prototype thermal energy storage tank using paraffin for space heating application. *Int. J. Thermofluids* **2020**, *1–2*, 100003. [[CrossRef](#)]
17. Dogkas, G.; Koukou, M.K.; Konstantaras, J.; Pagkalos, C.; Lymperis, K.; Stathopoulos, V.; Coelho, L.; Rebola, A.; Vrachopoulos, M.G. Investigating the performance of a thermal energy storage unit with paraffin as phase change material, targeting buildings' cooling needs: An experimental approach. *Int. J. Thermofluids* **2020**, *3–4*, 100027. [[CrossRef](#)]
18. Coelho, L.; Koukou, M.K.; Dogkas, G.; Konstantaras, J.; Vrachopoulos, M.G.; Rebola, A.; Benou, A.; Choropanitis, J.; Karytsas, C.; Sourkounis, C.; et al. Latent Thermal Energy Storage Application in a Residential Building at a Mediterranean Climate. *Energies* **2022**, *15*, 1008. [[CrossRef](#)]
19. DesignBuilder Software Ltd. DesignBuilder Help v7.0. Available online: <https://designbuilder.co.uk/helpv7.0/> (accessed on 23 September 2021).
20. Center of Renewable Energy Sources and Savings. *TESSe2b Deliverable 7.1—Performance Evaluation Report and Economic Feasibility Study of TESSe2b Solution Small Scale Validation in Austria*; Center of Renewable Energy Sources and Savings: Athens, Greece, 2019; Volume 1, pp. 1–35.
21. *TESSe2b Deliverable 4.3—Report on the Technical Characteristics of Enhanced PCM BHEs*; Geoteam S.A.: Graz, Austria, 2019; Volume 1, pp. 1–37.
22. Sanner, B.; Hellström, G.; Spitler, J.; Gehlin, S. Thermal Response Test—Current Status and World-Wide Application. In *Proceedings of the World Geothermal Congress 2005, Antalya, Turkey, 24–29 April 2005*; Available online: <https://www.geothermal-energy.org/pdf/IGAstandard/WGC/2005/1436.pdf> (accessed on 14 August 2023).
23. Vrachopoulos, M.G.; Koukou, M.K.; Tsolakoglou, N.P. Exploitation of Normal (Shallow) Geothermy for heating and cooling applications. In *Recent Advances in Renewable Energy Systems, Volume 3: Renewable Energy Engineering: Solar, Wind, Biomass, Hydrogen and Geothermal Energy System*; Rogdakis, E.D., Koronaki, I.P., Eds.; Bentham Science Publishers: Sharjah, United Arab Emirates, 2018; pp. 324–368.
24. PCM Products. Available online: [www.pcmproducts.net](http://www.pcmproducts.net) (accessed on 23 September 2021).
25. Pagkalos, C.; Koukou, M.K.; Vrachopoulos, M.G.; Konstantaras, J.; Dogkas, G.; Stylianou, S.; Stathopoulos, V.; Lymperis, K. Design of Thermoplastic Tanks for Thermal Energy Storage Applications Using Finite Element Analysis. In *Proceedings of the EinB2019-8th International Conference “Energy in Buildings 2019”, Athens, Greece, 28 September 2019*; Available online: [https://www.ashrae.gr/Proceedings/EinB2019\\_Proceedings.pdf](https://www.ashrae.gr/Proceedings/EinB2019_Proceedings.pdf) (accessed on 25 October 2023).

**Disclaimer/Publisher’s Note:** The statements, opinions and data contained in all publications are solely those of the individual author(s) and contributor(s) and not of MDPI and/or the editor(s). MDPI and/or the editor(s) disclaim responsibility for any injury to people or property resulting from any ideas, methods, instructions or products referred to in the content.